

# Dynamic crossover scaling in polymer solutions

Aashish Jain,<sup>1</sup> B. Dünweg,<sup>2,1</sup> and J. Ravi Prakash<sup>1,\*</sup>

<sup>1</sup>Department of Chemical Engineering, Monash University, Melbourne, VIC 3800, Australia

<sup>2</sup>Max Planck Institute for Polymer Research, Ackermannweg 10, 55128 Mainz, Germany

(Dated: November 11, 2018)

The crossover region in the phase diagram of polymer solutions, in the regime above the overlap concentration, is explored by Brownian Dynamics simulations, to map out the universal crossover scaling functions for the gyration radius and the single-chain diffusion constant. Scaling considerations, our simulation results, and recently reported data on the polymer contribution to the viscosity obtained from rheological measurements on DNA systems, support the assumption that there are simple relations between these functions, such that they can be inferred from one another.

PACS numbers: 83.80.Rs, 83.85.Jn, 83.10.Rs, 83.10.Mj, 47.57.Ng, 47.57.Qk, 83.60.Bc, 82.35.Lr, 05.10.Gg, 05.40.Jc

The basic physics of systems of linear flexible uncharged macromolecules in solution, in a wide range of concentrations and solvent qualities, can be considered as reasonably well understood, at least as far as the standard scaling laws are concerned, which govern the static and near-equilibrium dynamic properties of the solution [1–4]. The fairly rich structure of the generic phase diagram of this system [3, 4], shown in Fig. 1, is a result of the interplay between molecule-molecule overlap on the one hand, and solvent quality effects on the other. These factors determine whether excluded-volume (EV) interactions between monomers are important or not. For highly dilute systems, where overlap is unimportant, we may characterize the effective strength of the EV interaction (or quality of the solvent) by the dimensionless parameter  $z^* = (\epsilon/k_B T)(1 - \Theta/T)$ , where  $k_B$  is Boltzmann’s constant,  $T$  is the temperature,  $\Theta$  is the Theta temperature at which an isolated infinitely long chain would collapse, and  $\epsilon$  is the repulsive energy (of enthalpic origin) with which two monomers interact. For small  $z^*$ , EV effects are unimportant, and the chain conformations obey random-walk (RW) statistics ( $R \sim bN^{1/2}$ , where  $R$  is the size of the chain,  $N$  its number of monomers and  $b$  the monomer size), while for large  $z^*$  the chain is swollen and obeys the statistics of a self-avoiding walk (SAW),  $R \sim bN^\nu$ , where  $\nu \approx 0.6$  is the Flory exponent. Upon increasing the concentration  $c$  (number of monomers per unit volume) beyond the overlap value  $c^*$ , Flory screening sets in, such that for such systems again  $R \propto N^{1/2}$ , even in the case of a good solvent. This interplay is well described by the “blob” concept [1, 3, 4], where the thermal blob size  $\xi_T$  characterizes the length scale (in real space) up to which EV is unimportant due to an insufficiently large value of  $z^*$ , while the overlap (or concentration) blob size  $\xi_c$  is the typical length scale above which chain overlap induces Flory screening. A semidilute solution (regime C in Fig. 1) is characterized by  $b \ll \xi_T \ll \xi_c \ll R$ , i. e. by only a finite window of length scales between  $\xi_T$  and  $\xi_c$  where SAW statistics apply. Upon further increasing  $c$ , the system enters the concen-

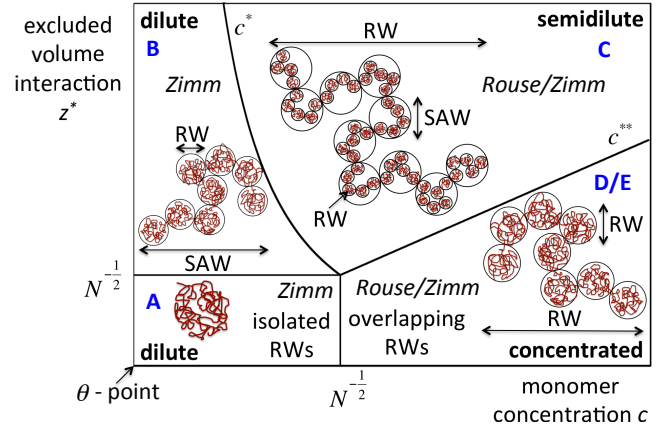


FIG. 1. (Color online) Phase diagram of a polymer solution in the plane monomer concentration  $c$  and excluded-volume strength  $z^*$ , as predicted by the standard blob picture. The  $\Theta$  regime occurs for small  $z^* \ll N^{-1/2}$ , while  $z^* \gg N^{-1/2}$  in the good solvent regime. The overlap concentration is given by  $c^*$ . For concentrations above  $c^*$ , excluded-volume interactions are completely screened. For derivations of relations governing the crossover boundaries, see Supplemental Material [5].

trated regime  $c \gg c^{**}$ , where this window has shrunk to zero. The lines drawn in Fig. 1 thus do not indicate sharp phase transitions but rather smooth crossovers.

These crossovers in the static conformational properties are accompanied by a dynamic crossover [1–4]. For  $c \ll c^*$ , hydrodynamic interactions (HI) are important, such that the dynamics is characterized by the scaling laws of the Zimm model (most notably  $D \sim k_B T / (\eta_s R)$ , where  $D$  is the single-chain diffusion constant, and  $\eta_s$  the solvent viscosity). For  $c \gg c^*$ , HI are screened, essentially as a result of chain-chain collisions which tend to randomize the momentum propagation in the system. The fact that HI in semidilute solutions are unscreened for short times [6] (up to the Zimm relaxation time of an overlap blob, which is the typical waiting time for chain-chain collisions to occur) is of no relevance for the present paper, since we are interested in the long-time dynamics

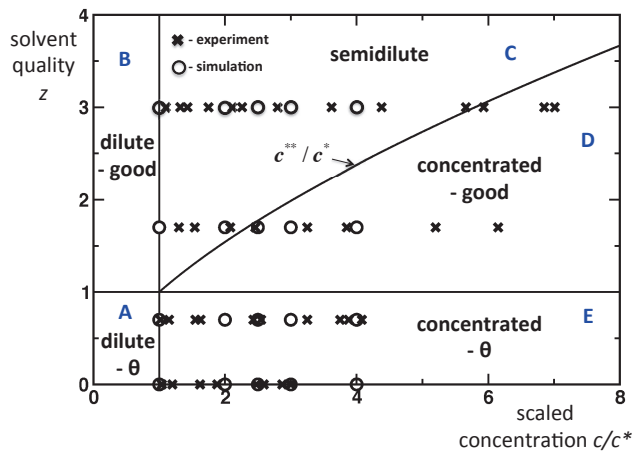


FIG. 2. (Color online) Same as Fig. 1 but with  $c/c^*$  and  $z = z^*N^{1/2}$  as variables. In this representation the loci of the crossovers do not depend on the chain length  $N$ . The points where the present simulations and recently reported experiments [12] have been performed are indicated as well.

only. Therefore here the scaling laws of the Rouse model (e. g.  $D \propto N^{-1}$ ) apply. We consider only systems where  $N$  and  $c$  are still small enough that entanglements play no essential role, such that a further crossover to reptation dynamics [1–4] does not need to be taken into account. HI screening is governed by the same length scale  $\xi_c$  as EV screening [6, 7].

Applying the blob picture to the various regimes of Fig. 1, one finds straightforwardly the scaling results for  $\xi_T$ ,  $\xi_c$ ,  $R$ ,  $D$ , and the polymer contribution to the viscosity  $\eta_p$ , listed in Table I of the Supplemental Material [5], and we refer the reader to the literature [4] for further details.

In the past, these scaling laws (which are asymptotic results applicable only sufficiently far away from the crossover regions), as well as the concentration-driven crossovers, have been subjected to a wealth of carefully executed experiments [4, 8] and computer simulations [6, 9]. However, to the best of our knowledge, there have been only few investigations that have tried to study the *double* crossover driven by both solvent quality and concentration, in particular when dynamic properties are concerned [10]. The present Letter attempts to fill that gap. We are particularly interested in the *universal* crossover scaling functions [11], which describe the behavior in the asymptotic limit  $N \rightarrow \infty$ .

The first step in analyzing universal crossover behavior is the introduction of suitably scaled dimensionless variables (or ratios). We therefore re-parameterize the scaling laws by replacing the EV strength  $z^*$  with the “solvent quality” parameter  $z = z^*N^{1/2}$  (note that this is the standard crossover scaling variable used to describe the  $\Theta$  transition), and the monomer concentration  $c$  with the

ratio  $c/c^*$ . The results of this transformation are shown in Fig. 2 and listed in Table I. For  $R$ ,  $D$  and  $\eta_p$  we introduce dimensionless ratios as indicated in the table. In this representation the dependence on the chain length  $N$  has been completely absorbed in the  $N$  dependence of  $c^*$  and  $z$ , and the only remaining variables are  $c/c^*$  and  $z$ . It is therefore natural to generalize these results to the relations  $R/R^* = \phi_R(c/c^*, z)$ ,  $D/D^* = \phi_D(c/c^*, z)$ , and  $\eta_p/\eta_p^* = \phi_\eta(c/c^*, z)$ , where  $R^*$ ,  $D^*$ ,  $\eta_p^*$  denote the values of  $R$ ,  $D$ ,  $\eta_p$  at  $c = c^*$ , and  $\phi_D$ ,  $\phi_R$ , and  $\phi_\eta$  are universal crossover scaling functions defined on the whole plane of Fig. 2, and which, up to numerical prefactors, are known deep in the asymptotic regimes (these are just the results listed in Table I), but whose behavior needs to be calculated or measured near the crossover lines.

An interesting observation can be made when looking at the last two lines of Table I. In all regimes above the overlap concentration, we find that the functions  $R/R^*$ ,  $D/D^*$ , and  $\eta_p/\eta_p^*$  are not independent, but can be calculated as soon as one of them is known. It is then natural to assume that the same property also holds in the crossover regimes, i.e. that the relations  $(c/c^*)^{1/4}\phi_R\phi_D^{1/4} = \text{const.}$  and  $(c/c^*)^{1/3}\phi_R\phi_\eta^{-1/6} = \text{const.}$  hold in the whole plane  $c/c^* \gg 1$  — or, in other words, that there is essentially only a single crossover scaling function in the problem.

In what follows, we present results for  $\phi_R$  and  $\phi_D$  obtained by careful computer simulations. It turns out that the convergence to the universal behavior is quite rapid, and can be treated fairly reliably by extrapolations [13]. In addition, we use recently reported data on  $\phi_\eta$  (obtained from rheological measurements on DNA systems) [12], to support the hypothesis of the existence of a single crossover scaling function. Due to the universality of our results, they should be broadly applicable to a large class of experimental systems.

A linear bead-spring chain model is used to represent polymer molecules, with each polymer chain coarse-grained into a sequence of  $N$  beads connected by massless springs. An ensemble of  $N_c$  such bead-spring chains, enclosed in a cubic cell of edge length  $L$  and immersed in an incompressible Newtonian solvent, is used to model the polymer solution. The monomer concentration of beads per cell is  $c = N_{\text{tot}}/V$ , where  $N_{\text{tot}} = N \times N_c$  is the total number of beads, and  $V = L^3$  is the volume of the simulation cell. A Brownian dynamics algorithm [14] which accounts for HI between the beads, and which can simulate both  $\Theta$  and good solvent conditions, is used here to obtain the stochastic time evolution of bead positions. In particular, the pair-wise EV interactions between beads  $\nu$  and  $\mu$  in a chain are represented by a narrow Gaussian potential [13, 15]

$$\frac{E(\mathbf{r}_{\nu\mu})}{k_B T} = z^* \left( \frac{1}{d^{*3}} \right) \exp \left\{ -\frac{1}{2b^2} \frac{\mathbf{r}_{\nu\mu}^2}{d^{*2}} \right\}, \quad (1)$$

regime	A	B	C	D	E
$\xi_T/(bN^{1/2})$	–	$z^{-1}$	$z^{-1}$	–	–
$\xi_c/(bN^{1/2})$	–	–	$(c/c^*)^{-\frac{1}{3\nu-1}} z^{2\nu-1}$	$(c/c^*)^{-1} z^{3(2\nu-1)}$	$(c/c^*)^{-1}$
$R/(bN^{1/2})$	1	$z^{2\nu-1}$	$(c/c^*)^{-\frac{1}{2} \frac{2\nu-1}{3\nu-1}} z^{2\nu-1}$	1	1
$D\eta_s bN^{1/2}/(k_B T)$	1	$z^{-(2\nu-1)}$	$(c/c^*)^{-\frac{1-\nu}{3\nu-1}} z^{-(2\nu-1)}$	$(c/c^*)^{-1} z^{3(2\nu-1)}$	$(c/c^*)^{-1}$
$\eta_p/\eta_s$	$c/c^*$	$c/c^*$	$(c/c^*)^{\frac{1}{3\nu-1}}$	$(c/c^*)^2 z^{-6(2\nu-1)}$	$(c/c^*)^2$
$R/R^*$	1	1	$(c/c^*)^{-\frac{1}{2} \frac{2\nu-1}{3\nu-1}}$	$z^{-(2\nu-1)}$	1
$D/D^*$	1	1	$(c/c^*)^{-\frac{1-\nu}{3\nu-1}}$	$(c/c^*)^{-1} z^{4(2\nu-1)}$	$(c/c^*)^{-1}$
$\eta_p/\eta_p^*$	$c/c^*$	$c/c^*$	$(c/c^*)^{\frac{1}{3\nu-1}}$	$(c/c^*)^2 z^{-6(2\nu-1)}$	$(c/c^*)^2$
$(c/c^*)^{1/4} (R/R^*) (D/D^*)^{1/4}$	$(c/c^*)^{1/4}$	$(c/c^*)^{1/4}$	1	1	1
$(c/c^*)^{1/3} (R/R^*) (\eta_p/\eta_p^*)^{-1/6}$	$(c/c^*)^{1/6}$	$(c/c^*)^{1/6}$	1	1	1

TABLE I. Various normalized quantities of the polymer system (thermal blob size  $\xi_T$ , overlap blob size  $\xi_c$ , polymer radius  $R$ , single-chain diffusion constant  $D$ , polymer part of the viscosity  $\eta_p$ ) in the regimes indicated in Fig. 2, in terms of  $c/c^*$  and  $z$ . Blob sizes are not indicated where they are irrelevant. Numerical prefactors of order unity have been ignored.  $R^*$ ,  $D^*$ ,  $\eta_p^*$  denote the values of  $R$ ,  $D$ ,  $\eta_p$  at  $c = c^*$ . For derivations, see Supplemental Material [5].

where  $d^*$  is a non-dimensional parameter that measures the range of excluded volume interaction,  $b$  is the monomer size, and  $\mathbf{r}_{\nu\mu}$  is the vector connecting monomers  $\nu$  and  $\mu$ . Simulations to explore the solvent quality crossover have been carried out by keeping the value of  $z$  constant at four different values:  $\{0, 0.7, 1.7, 3\}$ , with  $z = 0$  corresponding to  $\Theta$ -solutions. At each fixed value of  $z$ , values of  $c/c^*$  ranging from 0.1 to 4 have been used to sample both the dilute and semidilute regimes. The overlap concentration  $c^*$  is calculated from  $c^* = N/[(4\pi/3)R_{g0}^3]$ , where  $R_{g0}$  is the radius of gyration of a chain in the dilute limit, which is computed *a priori* by running *single chain* BD simulations. The box size  $L$  is selected to ensure  $L \geq 2R_e$  (where  $R_e$  is the end-to-end distance of a chain), in order to prevent a chain from wrapping over itself. For this purpose, the value of  $R_e$  at any value of  $c/c^*$  is estimated from the blob scaling law  $R_e = R_{e0} (c/c^*)^{-(2\nu-1)/(6\nu-2)}$  where  $R_{e0}$  is the end-to-end distance of a chain computed in the dilute limit. Typical simulations consist of an equilibration run for approximately one relaxation time followed by a production run of 10 to 60 relaxation times; here, the relaxation time  $\tau$  was estimated via  $\tau = R_g^2/(6D)$ , where  $R_g$  is the concentration-dependent radius of gyration. Moreover, data were obtained by averaging over 30 – 70 independent runs.

Asymptotic results at any point  $(c/c^*, z)$ , independent of simulation parameters, are obtained by accumulating finite chain data from BD simulations carried out at fixed values of these variables, and subsequently extrapolating to the limit  $N \rightarrow \infty$ . At finite values of  $N$ , the results still depend on the parameters  $d^*$  [see Eq. (1)], and on the hydrodynamic interaction parameter  $h^* = a/\sqrt{\pi(k_B T/H)}$ , where  $a$  is the bead radius and  $H$  is the spring constant. The parameter  $d^*$  is truly irrelevant in the long-chain limit, i.e. asymptotic conformation statistics are only governed by  $c/c^*$  and  $z$  [13]. Conversely,  $h^*$  is a variable similar to  $z^*$ , where the relevant scaling variable govern-

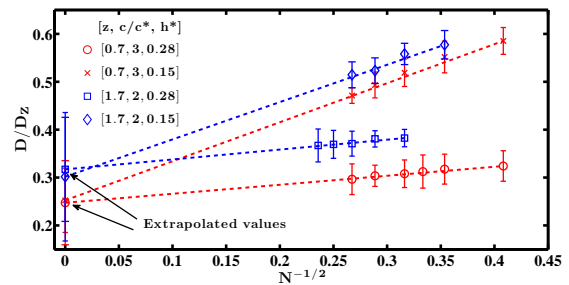


FIG. 3. (Color online) Universal predictions of the ratio  $D/D_Z$  at the two state points  $(z, c/c^*) = (0.7, 3)$  and  $(1.7, 2)$ , where  $D$  is the single-chain diffusion constant at the state point under consideration, while  $D_Z$  is the  $c = 0$  value at the same  $z$ . Data accumulated for finite chain lengths  $N$  (symbols) for two different values of the hydrodynamic interaction parameter ( $h^* = 0.15$  and  $0.28$ ) extrapolate to a unique value in the limit  $N \rightarrow \infty$ . The limited range of  $N$  values leads to a conservative estimate of the error of the extrapolated value.

ing the crossover from free-draining to non-draining behavior is the draining parameter  $h = h^*\sqrt{N}$  [13]. In the present study we focus on the non-draining limit  $h \rightarrow \infty$ , which is obtained by  $N \rightarrow \infty$  at constant  $h^*$ . This limit is independent of  $h^*$ , as demonstrated in Fig. 3 for  $D/D_Z$ , which is the ratio of the single-chain diffusion constant at a finite concentration to its value in the dilute limit. Data for chains of lengths  $N = 6$  to  $N = 20$  have been extrapolated to  $N \rightarrow \infty$ .

The resulting crossover scaling functions  $\phi_R(c/c^*, z)$  and  $\phi_D(c/c^*, z)$  are shown in Figs. 4, where the mean polymer size  $R$  is  $R_g$ . The data are limited to the crossover region where in principle none of the power laws of Table I hold. Since the observation regime is small, it is nevertheless possible to fit a power law to the data (without deeper theoretical justification). This gives rise to a convenient description in terms of an *effective* empirical

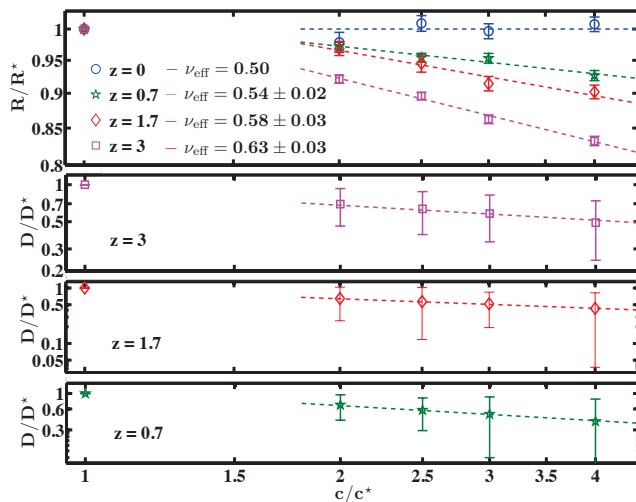


FIG. 4. (Color online) Concentration dependence of the crossover scaling functions  $\phi_R$  and  $\phi_D$  in the semidilute regime, for different values of solvent quality  $z$ , obtained by Brownian dynamics simulations. The effective exponents  $\nu_{\text{eff}}$  have been determined by fitting power laws to the data  $\phi_R \propto (c/c^*)^{-p}$  and requiring  $p = (2\nu_{\text{eff}} - 1)/(6\nu_{\text{eff}} - 2)$ , according to Table I in regime C. Using these values, lines are drawn according to  $\phi_D \propto (c/c^*)^{-q}$  with  $q = (1 - \nu_{\text{eff}})/(3\nu_{\text{eff}} - 1)$ .  $\phi_D$  data for  $z = 0$  are omitted because of large statistical errors.

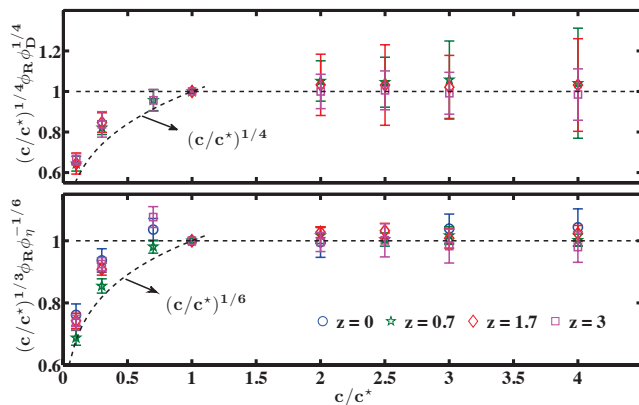


FIG. 5. (Color online) Demonstration that the functions  $R/R^*$ ,  $D/D^*$ , and  $\eta_p/\eta_p^*$  are not independent, but can be calculated as soon as one of them is known. In the upper panel,  $z = 0$  data are omitted because of large statistical errors.

exponent  $\nu_{\text{eff}}$  (for values see Figs. 4), which is obtained by adjusting the value of  $\nu$  in the scaling laws of regime C of Table I to the observed slope. Since the crossover scaling functions are related to each other (see below), each crossover yields the same value for  $\nu_{\text{eff}}$ . Moreover, consistency with the asymptotic laws requires that  $\nu_{\text{eff}}$  varies between 0.5 and 0.6. A similar crossover scaling behavior is obtained for  $\phi_\eta(c/c^*, z)$  from measurements

of  $\eta_p$  for semidilute DNA solutions across a range of  $N$ ,  $c$ , and  $z^*$  [12].

The validity of the expectation from scaling considerations that the combination  $(c/c^*)^{1/4} \phi_R \phi_D^{1/4} = 1$  in the entire semidilute regime, while it is proportional to  $(c/c^*)^{1/4}$  in the dilute limit, and similarly that the combination  $(c/c^*)^{1/3} \phi_R \phi_\eta^{-1/6} = 1$  in the entire semidilute regime and  $(c/c^*)^{1/6}$  in the dilute limit, is established in Figs. 5. In the case of the latter combination, while values of  $\phi_R$  have been obtained from the present simulations, values of  $\phi_\eta$  are from the data reported in Ref. 12. Clearly, the knowledge of a single two-argument scaling function is sufficient to describe the entire double crossover regime in polymer solutions.

\* Corresponding author: ravi.jagadeeshan@monash.edu; Visit: <http://users.monash.edu.au/~rprakash/>

- [1] P.-G. de Gennes, *Scaling Concepts in Polymer Physics* (Cornell University Press, Ithaca, 1979).
- [2] M. Doi and S. F. Edwards, *The Theory of Polymer Dynamics* (Clarendon Press, Oxford, New York, 1986).
- [3] A. Y. Grosberg and A. R. Khokhlov, *Statistical physics of macromolecules* (AIP Press, New York, 1994).
- [4] M. Rubinstein and R. H. Colby, *Polymer Physics* (Oxford University Press, 2003).
- [5] Supplemental Material at [URL will be inserted by publisher] for a summary and a brief derivation of the scaling laws.
- [6] P. Ahlrichs, R. Everaers, and B. Dünweg, Phys. Rev. E **64**, 040501 (2001).
- [7] P.-G. de Gennes, Macromolecules **9**, 594 (1976).
- [8] P. Wiltzius, H. R. Haller, D. S. Cannell, and D. W. Schaefer, Phys. Rev. Lett. **53**, 834 (1984); B. Ewen and D. Richter, Adv. Polym. Sci. **134**, 1 (1997).
- [9] W. Paul, K. Binder, D. W. Heermann, and K. Kremer, J. Phys. II France **1**, 37 (1991); M. Müller, K. Binder, and L. Schäfer, Macromolecules **33**, 4568 (2000); C.-C. Huang, R. G. Winkler, G. Sutmann, and G. Gompper, Macromolecules **43**, 10107 (2010).
- [10] P. J. Daivis and D. N. Pinder, Macromolecules **23**, 5176 (1990).
- [11] L. Schäfer, *Excluded Volume Effects in Polymer Solutions* (Springer-Verlag, Berlin, 1999).
- [12] S. Pan, D. A. Nguyen, P. Sunthar, T. Sridhar, and J. R. Prakash, “Universal solvent quality crossover of the zero shear rate viscosity of semidilute DNA solutions,” (2012), submitted to J. Rheol., arXiv:1112.3720v2 [cond-mat.soft].
- [13] M. Kröger, A. Alba-Pérez, M. Laso, and H. C. Öttinger, J. Chem. Phys. **113**, 4767 (2000); J. R. Prakash, Chem. Eng. Sci. **56**, 5555 (2001); K. S. Kumar and J. R. Prakash, Macromolecules **36**, 7842 (2003); P. Sunthar and J. R. Prakash, Macromolecules **38**, 617 (2005); Europhys. Lett. **75**, 77 (2006).
- [14] A. Jain, P. Sunthar, B. Dünweg, and J. R. Prakash, Phys. Rev. E **85**, 066703 (2012).
- [15] J. R. Prakash and H. C. Öttinger, Macromolecules **32**, 2028 (1999).

**Supplemental material for:  
Dynamic crossover scaling in polymer solutions**

Aashish Jain,<sup>1</sup> B. Dünweg,<sup>2,1</sup> and J. Ravi Prakash<sup>1,\*</sup>

<sup>1</sup>*Department of Chemical Engineering, Monash University, Melbourne, VIC 3800, Australia*

<sup>2</sup>*Max Planck Institute for Polymer Research, Ackermannweg 10, 55128 Mainz, Germany*

**BLOB SCALING IN THE CONCENTRATION  
AND SOLVENT QUALITY CROSSOVER  
REGIMES**

In regimes B and C of the phase diagram (see Fig. 1 in the main paper), where solvent quality effects play a role in determining the static and near-equilibrium dynamic properties of the solution, the length scale corresponding to thermal blobs is relevant. The size of the thermal blob  $\xi_T$  can be estimated as follows. Two monomers are assumed to interact with an energy  $\epsilon(1 - \Theta/T)$ ,  $T > \Theta$ ,  $\epsilon > 0$  — i. e. the interaction is repulsive. On small scales, the interaction is not strong enough to perturb the random-walk (RW) nature of the chain. The chain notices that there is repulsion only when the total repulsive energy is of order  $k_B T$ . This defines the thermal blob size, which we assume corresponds to  $n$  monomers. Since the number of contacts in a RW is of order  $n^{1/2}$  in three spatial dimensions, the condition to find  $n$  is

$$\epsilon \left(1 - \frac{\Theta}{T}\right) n^{1/2} = k_B T. \quad (1)$$

In the present work, the pair-wise excluded-volume (EV) interactions between monomers  $\nu$  and  $\mu$  in a chain are represented by a narrow Gaussian potential,

$$\frac{E(\mathbf{r}_{\nu\mu})}{k_B T} = z^* \left(\frac{1}{d^*}\right) \exp\left\{-\frac{1}{2b^2} \frac{\mathbf{r}_{\nu\mu}^2}{d^{*2}}\right\}, \quad (2)$$

where,  $d^*$  is a non-dimensional parameter that measures the range of excluded volume interaction,  $b$  is the monomer size, and  $\mathbf{r}_{\nu\mu}$  is the vector connecting monomers  $\nu$  and  $\mu$ . The parameter  $z^*$  is the non-dimensional strength of the pair-wise excluded-volume interactions. It follows that,

$$z^* = \frac{\epsilon}{k_B T} \left(1 - \frac{\Theta}{T}\right). \quad (3)$$

Equation (1) then implies,

$$n = (z^*)^{-2}. \quad (4)$$

The corresponding blob size is consequently

$$\xi_T = bn^{1/2} = b(z^*)^{-1}. \quad (5)$$

Using the definition of the solvent quality parameter,

$$z = z^* N^{1/2}, \quad (6)$$

where,  $N$  is the number of monomers in a chain, the non-dimensional blob size in terms of *scaled* variables is,

$$\frac{\xi_T}{bN^{1/2}} = z^{-1}. \quad (7)$$

In regimes B and C, on scales larger than  $\xi_T$  excluded volume is important. In regime B, where the monomer concentration  $c < c^*$ , the entire chain conformation is that of a self-avoiding walk (SAW) on length scales larger than  $\xi_T$ . However, in regime C, where  $c > c^*$ , Flory screening sets in at yet larger length scales leading to the existence of concentration blobs. Thermal blobs within the concentration blob obey SAW statistics. If  $\xi_c$  is the size of such a concentration blob, then its size is given by

$$\xi_c = \xi_T m^\nu, \quad (8)$$

where,  $\nu$  is the Flory exponent, while  $m$  is the number of thermal blobs within the concentration blob. The size  $\xi_c$  is found by the knowledge that the solution is homogeneous on scales larger than  $\xi_c$ , and that the concentration blobs are space filling. The total number of monomers within  $\xi_c$  is  $nm$ , therefore

$$nm = c \xi_c^3. \quad (9)$$

Using Eqs. (4), (8), and (5), it is straight forward to show that

$$m = (z^* c^{-1} b^{-3})^{1/(3\nu-1)}. \quad (10)$$

As a result, using Eqs. (5) and (10) in Eq. (8)

$$\xi_c = b(z^*)^{-\frac{2\nu-1}{3\nu-1}} (cb^3)^{-\frac{\nu}{3\nu-1}}. \quad (11)$$

In order to represent the size of the concentration blob in terms of scaled variables, it is necessary to calculate the overlap concentration  $c^*$ , which separates regimes B and C. The overlap concentration can be found from the condition that at  $c = c^*$ , the concentration blob contains just all monomers of the chain,  $N$ . From Eqs. (9), (8) and (5), since  $nm = N$  at  $c = c^*$

$$N = c^* b^3 z^{*-3} m^{3\nu}. \quad (12)$$

Substituting for  $m$  from Eq. (10), and solving for  $c^*$ , leads to

$$c^* = b^{-3} N^{-(3\nu-1)} z^{*-3(2\nu-1)}. \quad (13)$$

When solved for  $z^*$ , this leads to the equation of the line that separates regimes B and C in the unscaled variables phase diagram (Fig. 1 in the main paper).

It is convenient to represent  $cb^3$  as  $(c/c^*)(c^*b^3)$  when converting from unscaled to scaled variables. One can then show from Eqs. (11), (6) and (13) that the non-dimensional size of the concentration blob in terms of scaled variables is

$$\frac{\xi_c}{bN^{1/2}} = \left(\frac{c}{c^*}\right)^{-\nu/(3\nu-1)} z^{2\nu-1}. \quad (14)$$

Upon systematically increasing the concentration  $c$ , the concentration blob shrinks until at a threshold concentration  $c = c^{**}$ ,  $\xi_c = \xi_T$ , and there is then no longer any length scale where SAW statistics apply. The locus of points  $c^{**}$  separates regime C from regimes D and E in the unscaled variables phase diagram. It is straight forward to calculate  $c^{**}$  by equating Eqs. (5) and (11)

$$c^{**} = b^{-3} z^*. \quad (15)$$

In terms of scaled variables, it is similarly straight forward to show by equating Eqs. (7) and (14) that

$$c^{**} = c^* z^{2(3\nu-1)}. \quad (16)$$

In regimes D and E, where only RW statistics apply, the concentration blob size is given by

$$\xi_c = bg^{1/2}, \quad (17)$$

where,  $g$  is the number of monomers in a concentration blob. Since the solution is homogeneous on all length scales larger than  $\xi_c$ , and the concentration blobs are space filling,

$$c = \frac{g}{\xi_c^3} = \frac{g}{(bg^{1/2})^3}. \quad (18)$$

which implies

$$g = (cb^3)^{-2} \quad (19)$$

and as a result

$$\xi_c = b(cb^3)^{-1}. \quad (20)$$

The expression for  $c^*$  given by Eq. (13) is only valid away from the  $\Theta$  regime, *i.e.*, for  $z^* > N^{-1/2}$ . On the other hand, in the  $\Theta$  regime, since at  $c = c^*$  the concentration blob contains all the monomers in the chain, which implies  $\xi_c = bN^{1/2}$ , Eq. (20) leads to

$$c^* = b^{-3} N^{-1/2}. \quad (21)$$

This difference in the expressions for  $c^*$  makes it necessary to distinguish between regimes D (where EV effects are important) and E (where EV effects are negligible) when representing the size of the concentration blob (and

indeed all other observables) in terms of scaled variables. In regime D, Eqs. (20), (13) and (6) imply

$$\frac{\xi_c}{bN^{1/2}} = \left(\frac{c}{c^*}\right)^{-1} z^{3(2\nu-1)}, \quad (22)$$

while in regime E, Eqs. (20) and (21) imply

$$\frac{\xi_c}{bN^{1/2}} = \left(\frac{c}{c^*}\right)^{-1}. \quad (23)$$

Once the blob scaling laws for  $\xi_T$  are known in regimes B and C, and those for  $\xi_c$  are known in regimes C to E, the scaling laws for all other observables in these regimes can be derived. Even though these laws have been derived and discussed in detail previously [1–3], here, as examples, we derive the scaling laws for the static chain size  $R$ , and the single-chain diffusion coefficient  $D$ , in order to represent them in terms of the notation used in this work. The scaling laws for regime A are not discussed since the conventional notation in this regime is followed here. Once the expressions for  $R$  and  $D$  are known, the scaling laws for  $\eta_p$ , the polymer contribution to viscosity, can be derived from the relation  $\eta_p \sim k_B T (c/N) \tau$ , where  $\tau$  is the longest relaxation time of the macromolecule,  $\tau \sim R^2/D$ .

### Regime B

Since the chain obeys SAW statistics on length scales larger than  $\xi_T$ ,

$$R = \xi_T \left(\frac{N}{n}\right)^\nu. \quad (24)$$

Using Eqs. (4) and (5), leads to

$$R = bN^\nu (z^*)^{2\nu-1}. \quad (25)$$

The scaling relation in terms of scaled variables can be obtained by making use of Eq. (6)

$$\frac{R}{bN^{1/2}} = z^{2\nu-1}. \quad (26)$$

Zimm dynamics are relevant on all length scales. From the Nernst-Einstein relation,  $D = k_B T / \eta_s R$ , and Eq. (25)

$$D = \frac{k_B T}{\eta_s bN^\nu (z^*)^{2\nu-1}}, \quad (27)$$

where,  $\eta_s$  is the solvent viscosity. Defining a non-dimensional diffusion coefficient  $D/(k_B T / \eta_s bN^{1/2})$ , it follows from Eqs. (6) that it is given in terms of scaled variables by

$$\frac{D}{(k_B T / \eta_s bN^{1/2})} = z^{-(2\nu-1)}. \quad (28)$$

regime	A	B	C	D / E
$\xi_T$	–	$b(z^*)^{-1}$	$b(z^*)^{-1}$	–
$\xi_c$	–	–	$b(z^*)^{-\frac{2\nu-1}{3\nu-1}}(cb^3)^{-\frac{\nu}{3\nu-1}}$	$b(cb^3)^{-1}$
$R$	$bN^{1/2}$	$bN^\nu(z^*)^{2\nu-1}$	$bN^{1/2}[z^*(cb^3)^{-1}]^{\frac{1}{2}\frac{2\nu-1}{3\nu-1}}$	$bN^{1/2}$
$D$	$\frac{k_B T}{\eta_s b N^{1/2}}$	$\frac{k_B T}{\eta_s b N^\nu (z^*)^{2\nu-1}}$	$\frac{k_B T}{\eta_s b N} (z^*)^{-2\frac{2\nu-1}{3\nu-1}} (cb^3)^{-\frac{1-\nu}{3\nu-1}}$	$\frac{k_B T}{\eta_s b N} (cb^3)^{-1}$
$\eta_p$	$\eta_s c b^3 N^{1/2}$	$\eta_s c b^3 N^{3\nu-1} (z^*)^{3(2\nu-1)}$	$\eta_s (cb^3)^{\frac{1}{3\nu-1}} N (z^*)^{\frac{2\nu-1}{3\nu-1}}$	$\eta_s (cb^3)^2 N$

TABLE I. Various quantities of the polymer system (thermal blob size  $\xi_T$ , overlap blob size  $\xi_c$ , polymer radius  $R$ , single-chain diffusion constant  $D$ , polymer part of the viscosity  $\eta_p$ ) in the regimes indicated in Fig. 1 of the main paper, as a function of monomer size  $b$ , chain length  $N$ , excluded-volume interaction strength  $z^*$ , thermal energy  $k_B T$ , solvent viscosity  $\eta_s$ , and monomer concentration  $c$ , within the framework of scaling theory. Blob sizes are not indicated in cases where they are irrelevant. Numerical prefactors of order unity have been ignored. The scaling laws are valid in the asymptotic regimes sufficiently far away from the crossover boundaries.

### Regime C

Since RW statistics are obeyed on length scales larger than  $\xi_c$

$$R = \xi_c \left( \frac{N}{nm} \right)^{1/2}, \quad (29)$$

where,  $N/nm$  is the number of concentration blobs in a chain. Using Eqs. (4), (10) and (11), leads to

$$R = bN^{1/2} [z^*(cb^3)^{-1}]^{\frac{1}{2}\frac{2\nu-1}{3\nu-1}}. \quad (30)$$

The scaling relation in terms of scaled variables is obtained by using Eqs. (6) and (13)

$$\frac{R}{bN^{1/2}} = \left( \frac{c}{c^*} \right)^{-\frac{1}{2}\frac{2\nu-1}{3\nu-1}} z^{2\nu-1}. \quad (31)$$

Rouse dynamics are obeyed on length scales larger than  $\xi_c$ . Therefore

$$D = \frac{k_B T}{\eta_s \xi_c (N/nm)}. \quad (32)$$

Using Eqs. (4), (10) and (11), leads to

$$D = \frac{k_B T}{\eta_s b N} (z^*)^{-2\frac{2\nu-1}{3\nu-1}} (cb^3)^{-\frac{1-\nu}{3\nu-1}}. \quad (33)$$

The non-dimensional diffusivity in terms of scaled variables follows from using Eqs. (6) and (13) in Eq. (33)

$$\frac{D}{(k_B T/\eta_s b N^{1/2})} = (c/c^*)^{-\frac{1-\nu}{3\nu-1}} z^{-(2\nu-1)}. \quad (34)$$

### Regime D

In regime D, RW statistics are obeyed on all length scales, both within the concentration blob, and by the concentration blobs themselves. As a result

$$R = \xi_c \left( \frac{N}{g} \right)^{1/2} = bN^{1/2}, \quad (35)$$

where Eqs. (19) and (20) have been used for simplification. The non-dimensional chain size is trivially  $R/(bN^{1/2}) = 1$ .

Rouse dynamics are obeyed on length scales larger than  $\xi_c$ . Using Eqs. (32) (with  $g = nm$ ), and Eqs. (19) and (20) leads to

$$D = \frac{k_B T}{\eta_s b N} (cb^3)^{-1}. \quad (36)$$

The non-dimensional diffusivity in terms of scaled variables follows from Eqs. (6) and (13)

$$\frac{D}{(k_B T/\eta_s b N^{1/2})} = \left( \frac{c}{c^*} \right)^{-1} z^{3(2\nu-1)}. \quad (37)$$

### Regime E

In regime E, the scaling relations for  $R$  and  $D$  in terms of unscaled variables are identical to those in regime D, since in both regimes, RW statistics are obeyed on all length scales, and Rouse dynamics apply on length scales larger than  $\xi_c$ . In terms of scaled variables, while the distinction between the two regimes is irrelevant for the static chain size, the difference in the expression for  $c^*$  due to the presence and absence of EV effects, respectively, manifests itself as a difference in the expression for the non-dimensional diffusivity. Using Eqs. (6) and (21), Eq. (36) reduces in terms of scaled variables to

$$\frac{D}{(k_B T/\eta_s b N^{1/2})} = \left( \frac{c}{c^*} \right)^{-1}. \quad (38)$$

Table I summarises all the unscaled equations derived in this section, including those for the polymer contribution to viscosity. Table I in the main paper summarises the equations in terms of scaled variables.

## ESTIMATION OF THE ERROR IN THE DIFFUSION COEFFICIENT $D$

### Error at finite $N$

The long time self-diffusion coefficient is calculated from the mean-square displacement (MSD) of the center of mass of each chain [4]. Each stochastic trajectory in the simulation leads to a time series for the MSD. An ensemble average over all the trajectories then gives the time series of the mean of the MSD (denoted here as  $\text{MSD}_{\text{avg}}$ ). Since the initial  $\text{MSD}_{\text{avg}}$  data represents transient short time diffusivity, while the data at large times have large error bars (they are based on a smaller number of blocks in the block averaging method), we typically discard the first 15 – 20% and last 20 – 30% of the data. This leads to a window of times  $\Delta\tau$  in the  $\text{MSD}_{\text{avg}}$  data that can be fitted with a straight line. At a given value of  $N$ , the size of  $\Delta\tau$  depends on the state point  $(z, c/c^*)$ . For a fixed set of parameters, the slopes of the lines fitted to each of the MSD trajectories in the ensemble, over the range of times  $\Delta\tau$ , is used here to obtain an ensemble of predicted diffusion coefficients. The mean diffusion coefficient  $D$  and the standard error of mean is then determined from this ensemble.

### Error in the extrapolated value at $N \rightarrow \infty$

At each state point  $(z, c/c^*)$  the mean value of  $D$  and the error in the mean, for a set of finite size chains with  $N = 6, 8, \dots, 20$ , is obtained as described above. The mean and error-of-mean of the ratio  $D/D_Z$  is then obtained via single chain BD simulations to determine  $D_Z$  for the same values of  $N$  and  $z$ . As described in the main paper, the asymptotic value of  $D/D_Z$  in the long chain limit is obtained by plotting the data at finite  $N$  as a function of  $N^{-1/2}$ , and extrapolating a straight line fit to the data, to the limit  $N \rightarrow \infty$ . The fitting of the straight line, and the estimation of the error in the extrapolated value is carried out here with the help of “Least-Squares Fitting” numerical routines provided in the GNU Scientific Library (GSL).

Essentially, the GSL routine finds the least-squares fit by minimizing  $\chi^2$ , the weighted sum of squared residuals, for the straight line model  $D/D_Z = c_0 + c_1 N^{-1/2}$ . The weights are the inverse of the error at each data point. The fitting routine `gsl_fit_wlinear` returns the best-fit parameters  $c_0$  and  $c_1$ , along with a  $2 \times 2$  covariance matrix that measures the statistical errors on  $c_0$  and  $c_1$  resulting from the errors in the data. The standard deviations of the best-fit parameters are then given by the square root of the corresponding diagonal elements of the covariance matrix. Particularly conveniently, the routine `gsl_fit_linear_est` uses the best-fit coefficients  $c_0$ ,  $c_1$  and their estimated covariance to compute the fitted func-

tion and its standard deviation at any desired point. By using `gsl_fit_linear_est` to find the value of the fitted function and its error at  $N^{-1/2} = 0$ , we determine both the infinite chain length limit value of  $D/D_Z$  and its associated error.

### SCALING OF COMPUTATIONAL COST WITH CHAIN SIZE

As illustrated in Fig. 3 of the main paper, asymptotic predictions in the long chain limit have been obtained for each state point  $(z, c/c^*)$  by extrapolating finite chain data accumulated for chain lengths ranging from  $N = 6$  to  $N = 20$ . The use of this rather limited range of  $N$  values is necessitated by the computational cost of the Brownian dynamics simulation algorithm used here. As shown below, an estimate of the computational cost of the algorithm can be derived by using some simple scaling arguments, and the resulting expression can be verified by comparison with the CPU time required in the current simulations.

The computational cost of carrying out an Euler integration of the governing stochastic differential equation for a single time step has been shown in Ref. 4 to scale with system size as  $N_{\text{tot}}^x$ , where  $x = 2.1$ . Recall that  $N_{\text{tot}} = N \times N_c$  is the total number of beads in a cubic cell of edge length  $L$ , with  $N_c$  being the number of bead-spring chains. Since typical simulations consist of runs extending over several relaxation times  $\tau$ , followed by averaging over many independent runs, it is necessary to find the dependence of  $\tau$  on  $N$  in order to find the scaling of the total CPU cost. This is done as follows for simulations carried out in the semidilute regime C.

From Eq. (31), the requirement that  $L \geq 2R$  in order to prevent chains from wrapping over themselves leads to

$$L \sim b \left( \frac{c}{c^*} \right)^{-\frac{1}{2} \frac{2\nu-1}{3\nu-1}} z^{2\nu-1} N^{1/2}. \quad (39)$$

The concentration of monomers in the simulation box is  $c = (NN_c)/L^3$ . As a result, from Eq. (39)

$$c \sim \left( \frac{N_c}{b^3} \right) \left( \frac{c}{c^*} \right)^{\frac{3}{2} \frac{2\nu-1}{3\nu-1}} z^{-3(2\nu-1)} N^{-1/2}. \quad (40)$$

Using Eqs. (13) and (6), the overlap concentration  $c^*$  can be written in terms of the solvent quality  $z$  as

$$c^* \sim b^{-3} z^{-3(2\nu-1)} N^{-1/2}. \quad (41)$$

It follows from Eqs. (40) and (41) that  $N_c$  is independent of  $z$ , and related to the scaled concentration through the relation

$$N_c \sim \left( \frac{c}{c^*} \right)^{\frac{1}{2} \frac{1}{3\nu-1}}. \quad (42)$$



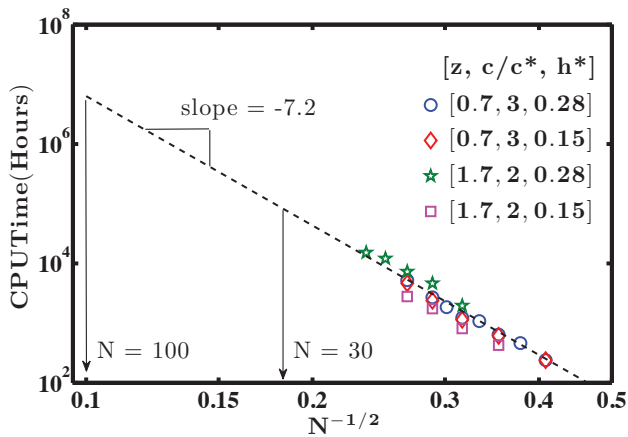


FIG. 1. (Color online) CPU time as a function of chain length for Brownian dynamics simulations carried out at the two state points  $(z, c/c^*) = (0.7, 3)$  and  $(1.7, 2)$  for two different values of the hydrodynamic interaction parameter ( $h^* = 0.15$  and  $0.28$ ), on a 156 SGI Altix XE 320 cluster. Symbols represent the various values of chain length  $N$  used in the simulations, while the dashed line is drawn with a slope predicted by the scaling relation Eq. (44).

The number of chains in a simulation box is consequently *constant* when  $(c/c^*)$  is maintained constant.

The relaxation time of a macromolecule  $\tau \sim R^2/D$ . From Eqs. (31) and (34), this implies

$$\tau \sim \tau_0 (c/c^*)^{\frac{2-3\nu}{3\nu-1}} z^{3(2\nu-1)} N^{3/2}. \quad (43)$$

where  $\tau_0 = \eta_s b^3/k_B T$  is the monomer relaxation time.

The total computational cost of a single stochastic trajectory consequently scales as  $\tau (N_c N)^x$ . For fixed values of  $z$  and  $(c/c^*)$  therefore

$$\text{Total CPU time per run} \sim N^{\frac{3}{2}+x} \sim \left(N^{-\frac{1}{2}}\right)^{-7.2} \quad (44)$$

where in the last expression on the right-hand-side we have substituted the value  $x = 2.1$  for the current algorithm, and used an exponent for  $N$  that enables a representation of the CPU cost as displayed in Fig. 1.

The various symbols in Fig. 1 represent simulations carried out at the two state points  $(z, c/c^*) = (0.7, 3)$

and  $(1.7, 2)$ , for two different values of the hydrodynamic interaction parameter  $h^*$ , on a 156 SGI Altix XE 320 cluster. The simulations are identical to those used to display the ratio  $D/D_Z$  in Fig. 3 of the main paper. It is immediately apparent that the prediction in Eq. (44) for the scaling of the total CPU time with chain size is obeyed closely by the present simulations, independent of solvent quality and scaled concentration.

It is clearly desirable to add data for longer chains in order to improve the accuracy of the asymptotic value obtained by extrapolation to the long chain limit. Unfortunately, the additional CPU cost this would entail (which can be estimated from the scaling of computational cost with chain size shown in Fig. 1) makes this highly infeasible. For instance, simulating a chain with  $N = 30$  would require roughly  $\mathcal{O}(10^4)$  CPU hours, while  $N = 100$  would require roughly  $\mathcal{O}(10^6)$  CPU hours! Indeed, by including simulations for a chain with  $N = 30$ , the CPU time for obtaining the static and dynamic properties of a semidilute solution at a single state point  $(z, c/c^*) = (3, 4)$  in the phase diagram (Fig. 2 of the main paper) is estimated to increase from its current value of approximately  $7 \times 10^4$  hours to roughly  $3 \times 10^5$  hours.

The authors gratefully acknowledge CPU time grants from the National Computational Infrastructure (NCI) facility hosted by Australian National University, and Victorian Life Sciences Computation Initiative (VLSCI) hosted by University of Melbourne.

---

\* Corresponding author: ravi.jagadeeshan@monash.edu; Visit: <http://users.monash.edu.au/~rprakash/>

- [1] P.-G. de Gennes, *Scaling Concepts in Polymer Physics* (Cornell University Press, Ithaca, 1979).
- [2] A. Y. Grosberg and A. R. Khokhlov, *Statistical physics of macromolecules* (AIP Press, New York, 1994).
- [3] M. Rubinstein and R. H. Colby, *Polymer Physics* (Oxford University Press, 2003).
- [4] A. Jain, P. Sunthar, B. Dünweg, and J. R. Prakash, Phys. Rev. E **85**, 066703 (2012).